Silicon (2019) 11:39–49
https://doi.org/10.1007/s12633-018-9880-6

ORIGINAL PAPER

Physico-mechanical and Surface Wear Assessment of Magnesium Oxide Filled Ceramic Composites for Hip Implant Application

Chandramani Goswami[1] · I. K. Bhat[2] · Sivaiah Bathula[3] · Tej Singh[4] · Amar Patnaik[1]

Received: 13 February 2018 / Accepted: 23 April 2018 / Published online: 5 May 2018
© Springer Science+Business Media B.V., part of Springer Nature 2018

Abstract
In the present study, applicability of ceramic composites as ceramic-on-ceramic hip prostheses is explored. Hence, ceramic composites containing zirconium oxide, silicon nitride, chromium oxide by varying proportion of aluminum oxide and magnesium oxide were prepared by spark plasma sintering and subsequently characterized for their physico-mechanical and tribological properties. The physico-mechanical and tribological properties of the fabricated composites were evaluated by measuring their density, void content, indentation response, fracture toughness and wear resistance respectively. The mechanical properties and wear performance of the composites are significantly improved with the addition of magnesium oxide content. Experimental results indicated that the 3 wt.% magnesium oxide based hip implant composite showed highest hardness, highest fracture toughness, highest young's modulus with lowest wear rate. A maximum increase of approximately 44% in nanohardness, 14% in Young's modulus, 98% in fracture toughness and 75% in wear resistance are achieved by introducing 3 wt.% magnesium oxide content. The experimental results indicated that fabricated ceramic composites will stand out as a promising material for hip implant substitution.

Keywords Ceramic composite · Hip implants · Ceramic-on-ceramic hip prostheses · Wear

1 Introduction

Designing of high quality hip implant composites is the key problem to be solved in the contemporary world, which not only needs to choose and combine proper raw materials, but also makes hip implant composites getting some excellent performances such as low wear rate, excellent mechanical and biocompatible properties [1]. To achieve these performance requirements, numerous material combinations have been introduced for the development of hip implant composites. Some examples of these combinations are metal-on-polymer, ceramic-on-polymer, metal-on-metal, ceramic-on-metal and ceramic-on-ceramic [2]. The use of ceramic-on-ceramic composites have proved to be very efficient and have grown in popularity for hip replacement in the last decade [3]. This is due to the lower wear rates of these composites as compared to conventional metal-on-metal and metal-on-polymer composites [4, 5].

The wear debris of these composites reduces the possible reaction with surrounding tissue [6]. Moreover, the released wear debris is bio-inert and overcomes the commonly reported risk of cancerous metal ions production in metal-on-metal composites and osteolysis risk in metal-on-polymer composites [6–8]. The interest in ceramic-on-ceramic is also elevated due to improved mechanical properties and superior biocompatibility [9]. The first use of alumina in ceramic-on-ceramic hip replacement was reported by Boutine et al. [10]. The main reason of alumina preference was the formation of lesser wear debris (i.e. lower wear rate) which also lowered the risk of osteolysis. Conversely, alumina is a brittle material and has a small but persistent chance of fracture as reported by Iwakiri et al. [11]. To overcome this problem, various ceramic materials such as zirconium oxide, silicon nitride, chromium oxide etc. were reported to improve the fracture toughness and wear rate of alumina based hip implant composites.

✉ Amar Patnaik
apatnaik.mech@mnit.ac.in

1 Department of Mechanical Engineering, MNIT Jaipur, Jaipur 302017, India

2 Applied Mechanics Department, MNNIT Allahabad, Allahabad 211004, India

3 CSIR-National Physical Laboratory, New Delhi 110012, India

4 Department of Mechanical Engineering, Manav Bharti University, Solan 173229, India

Zirconium oxide is a non-cytotoxic, biocompatible and having three times higher flexural strength than alumina was used to improve mechanical properties and wear resistance of alumina based hip implant composites [12].

In this regard, while studying the wear rate of various ceramic combinations for hip replacement, a lower wear rate for zirconium oxide toughened alumina and alumina toughened zirconium oxide was reported by Al-Hajjar et al. [13]. Moreover, improvement in mechanical properties and wear resistance was also reported for chromium oxide filled alumina composites [14]. Silicon nitride, which has approximately 54% higher fracture toughness compared to zirconium oxide toughened alumina was also reported to be used in implant applications [15]. Mazzocchi and Bellosi [16, 17] demonstrate that implants made of silicon nitride exhibits excellent mechanical, wear and biocompatible qualities. The research outcomes suggested that silicon nitride may serve as a biomaterial for bone substitution in load bearing prosthesis. While studying the wear performance of silicon nitride based composites, Olofsson et al. [18] suggested that silicon nitride will prove a good material for hip replacement.

In another independent study, Pettersson et al. [19] concluded that silicon nitride coatings on cobalt chromium molybdenum alloy reduces the release of metal ions and potentially used for joint replacements. It was reported in literature that stresses on the zirconia surface resulting in its phase change which leads in grains expansion and thus led to degradation of materials properties [12]. Therefore, magnesium-oxide was reported to be used as a stabilizing oxide during the pre-sintering stage to seals the crack [20]. Magnesium oxide based composite nanofibers were also being reported to be used in tissue engineering applications by Rijal et al. [21]. The beneficial effect of stearic acid-modified magnesium oxide whiskers on the mechanical properties of polylactic acid based composites was reported by Zhao et al. [22]. It was claimed that inclusion of 1 wt.% modified magnesium oxide content in polylactic acid resulted in 78% and 17% increase in Young's modulus and tensile strength respectively. Recently biosynthesized magnesium oxide nanorods were also reported to exhibits anticancer, antibacterial activities which highlighting its biocompatible nature [23]. Zhang et al. [24] studied the mechanical properties, phase stability and biocompatibility of magnesium oxide and aluminum oxide based artificial joints composite. The hardness, flexural strength and fracture toughness of the fabricated composite reached to their maximum values of 17.5 GPa, 703 MPa and 12.1 $MPam^{1/2}$ respectively for 0.2 wt.% magnesium oxide based composites. The composites show good chemical stability and excellent biocompatibility. They also claimed that 0.2 wt.% magnesium oxide based composites can be used as wear-resistant artificial joint materials.

The ceramic-on-ceramic hip implant composites are well documented and magnesium oxide has been also reported to be used in biomedical applications. Hence, magnesium-oxide based ceramic-on-ceramic hip implant composites may potentially offer enhanced mechanical properties and wear resistance. Keeping this in mind, in current research work, the applicability of magnesium oxide as a potential reinforcement to improve the mechanical and wear properties of ceramic-on-ceramic composites for hip implant applications is explored. Hence, ceramic-on-ceramic composites containing zirconium oxide, silicon nitride, chromium oxide and varying proportion of aluminum oxide and magnesium oxide were developed and evaluated for their mechanical and wear properties.

2 Experimental Details

2.1 Materials and Fabrication Detail

The powders of commercial Al_2O_3 (Aluminum oxide), ZrO_2 (Zirconium oxide), Si_3N_4 (Silicon nitride), Cr_2O_3 (Chromium oxide) and MgO (Magnesium oxide) were purchased from Daisy Impex Chemicals, Delhi. The average particle size of the selected powder was in the range of 5–10 μm and all had purities in excess of 99.5%. The compositional details and corresponding composite designation are described in Table 1. Prior to sintering, 20 g of selected powders were milled by ball milling machine for 4 h in a tungsten vial using tungsten grinding media in 50 ml Toluene solution with a ball: powder ratio of 10:1 at 300 rpm. This mixture was separated, oven-dried and used for sintering process. The sintering was performed under the temperature conditions revealed in Fig. 1. The sintering temperature was set at 1400 °C with a uni-axial pressure of 60 MPa, heating rate of 300 °C per minute under vacuum (6 Pa). Sintered samples are approximately 20 mm in diameter and 10 mm thick. Afterwards, samples were grounded, polished (silicon carbide papers and diamond suspension) and ultrasonically cleaned in acetone for further characterization.

Table 1 Compositional details and designation of the hip implant composites

Designation	Composition (wt.%)				
	Al_2O_3	ZrO_2	Si_3N_4	Cr_2O_3	MgO
MO-1	73.5	20	5	1.5	0.0
MO-2	72.0	20	5	1.5	1.5
MO-3	70.5	20	5	1.5	3.0
MO-4	69.0	20	5	1.5	4.5

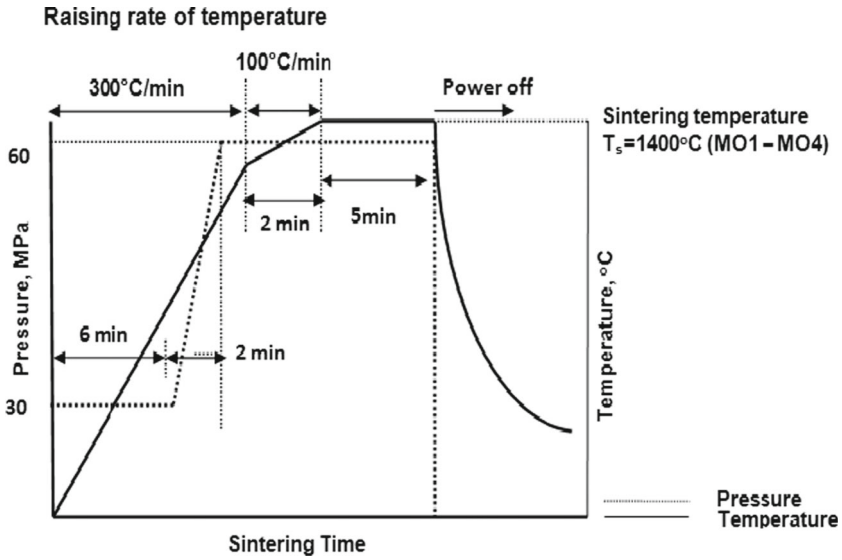

Fig. 1 Spark plasma sintering (SPS) process conditions

2.2 Physical and Mechanical Characterization

The XRD patterns of the fabricated ceramic hip implant composites were analyzed by a Panalytical X-ray (X'Pert3 Powder, Netherland) diffractometer instrument operating at a voltage of 45 kV and a current of 40 mA with Cu Ka radiation. The composites were scanned in the 2θ ranges 20° to 80° in the continuous scan mode. The surface morphology and elemental mapping of the fabricated hip implant composites were characterized by field emission scanning electron microscope (FESEM, Zeiss, SUPRA 40VP). For elemental analysis, energy dispersive X-ray (EDX) spectroscopy was performed on the same FESEM fitted with EDX analyzer. The nano-indentation measurements were performed using a Hysitron TI 750-D Ubi-1 model as per Oliver and Pharr's method [25]. Nano-indentation is represented as load-displacement plots of indentations performed at 5000 μN indentation-load (500 μN/s loading rate with a dwell time of 2 s at maximum load) on the fabricated composites. A Berkovich indenter having a pyramidal shape possessing a phase angle of 65.35 and edge to opposite side angle of 142.35 and tip radius of 150 nm was utilized in all experiments. For density measurement standard water displacement method was used whereas void content were calculated by normalizing of experimental density with respect to the theoretical density. For fracture toughness analysis, the polished composite surfaces were firstly penetrated by a pyramidal indenter for crack generation. So indentation load of 20N for 13 s duration was used for creating a deformed area underneath and in the surroundings of indentation. For indentations a hardness tester (1600–1000 indenter, Buehler, Lke Bluff IL) was used while the generated cracks were measured using an FESEM (Zeiss, SUPRA 40VP). The Anstis model [26] is used for fracture toughness (K_{IC}) calculation as:

$$K_{IC} = 0.016 \left(\frac{E}{H}\right)^{\frac{1}{2}} \times \frac{p}{c^{\frac{3}{2}}} \quad (1)$$

Where P is the applied load, E is Young's modulus, H is the hardness, and c is the length of the surface trace of the half penny crack measured from the center of the indent. For physical and mechanical characterization, the experiments are repeated five times and an average value of the results were reported.

2.3 Wear Characterization

The wear performance of the fabricated hip implant composites were evaluated using a ring on plate type tribometer (Fig. 2, TR-6474, Ducom Instruments, India) as per ISO 6474-1:2010 standard [27]. A cylindrical sized (20 mm × 10 mm) hip implant composite specimen was hydraulically compressed to the upper plate whereas the lower plate of size (25 mm × 6 mm) was made of MO-3. The upper plate was rotated through an arc of ±25° at frequency of 100 Hz whereas lower plate remains fixed. Wear tests were conducted for one million cycles at constant frequency in simulated body fluid lubricant which was prepared according to ISO 23317 [28]. For each specimen, the experiments are repeated thrice. The volumetric wear of the fabricated composite was determined by assessing the difference in weight before and after the testing procedure followed by normalization with the experimental density of the respected composite.

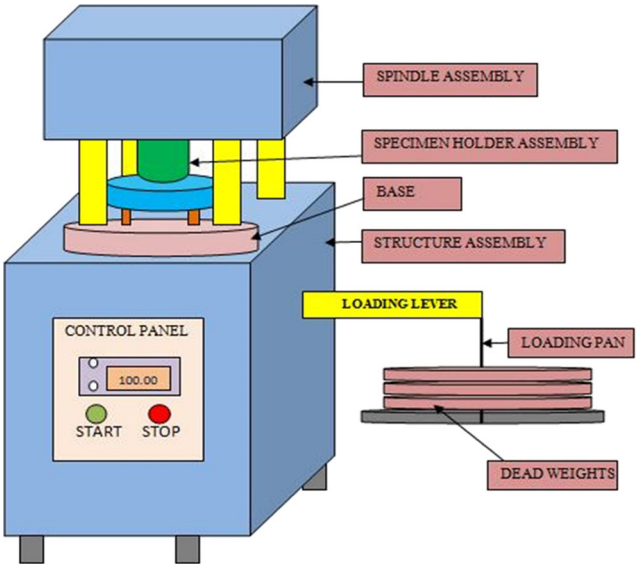

Fig. 2 Ring on plate tribometer

3 Result and Discussion

3.1 XRD Study

The XRD analysis of the fabricated hip implant composites is presented in Fig. 3. It can be seen that all the ingredients exhibits the same XRD pattern as described in JCPDS file. The peaks in XRD pattern of MgO filled composites was observed at $2\theta \sim 43.20$, which is according to JCPDS 78-0430 data file. It is reported in literature that many new materials such as aluminum oxycarbides may be formed as a result sintering process [29]. The XRD pattern clearly reveals that there is no new phase present in the composites.

3.2 FESEM and EDX Analysis

The FESEM were performed for microstructure analysis, elemental mapping and EDX analysis and shown in Figs. 4 and 5. From the EDX spectrums of fabricated composites, as shown in Fig. 3, it is clear that the constituents of fabricated hip implant composites i.e. O, Al, Si, Zr, Mg, Cr, N elements are present and no other elements were detected in the composites. Further from the elemental mapping spectrum of MO-3 (Fig. 4), it can be seen that the composite constituents are uniformly distributed.

3.3 Physico-Mechanical Properties

Investigated physical and mechanical properties of the fabricated hip implant composites are presented in Figs. 6, 7, 8, 9 and 10. As seen from Fig. 6, the density (4.154 ± 0.004 g/cm^3) of the composites remains almost constant

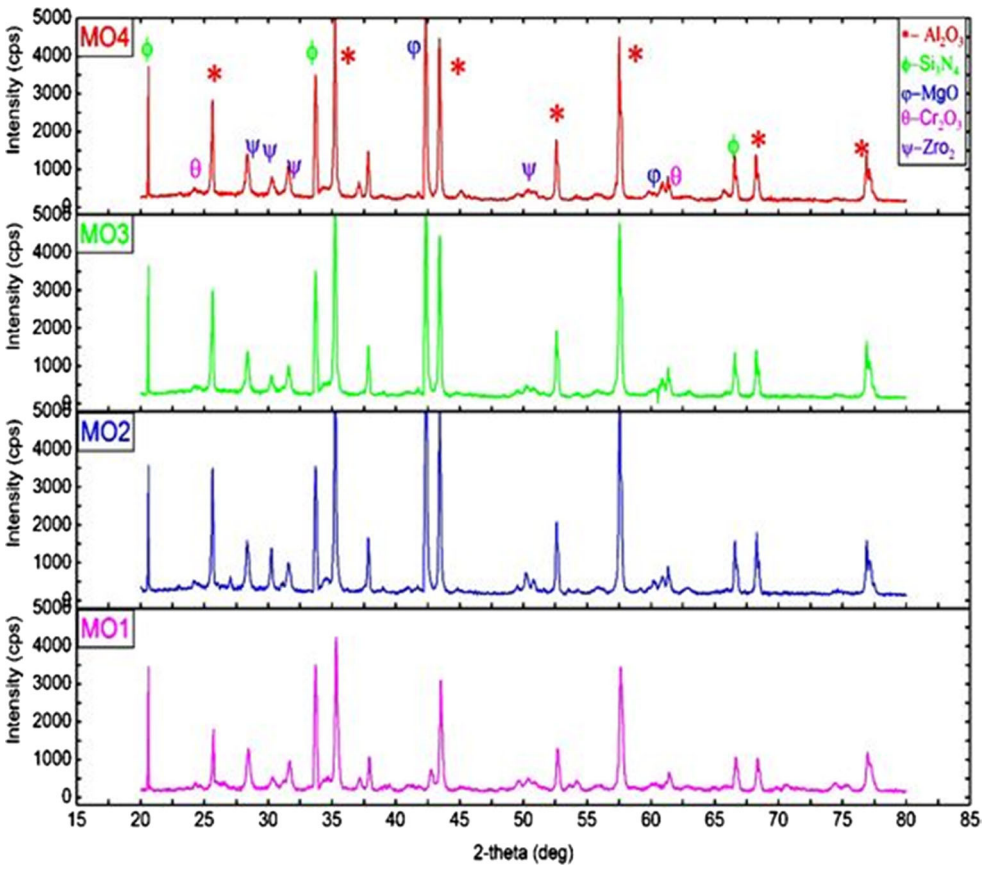

Fig. 3 XRD pattern of as sintered composites

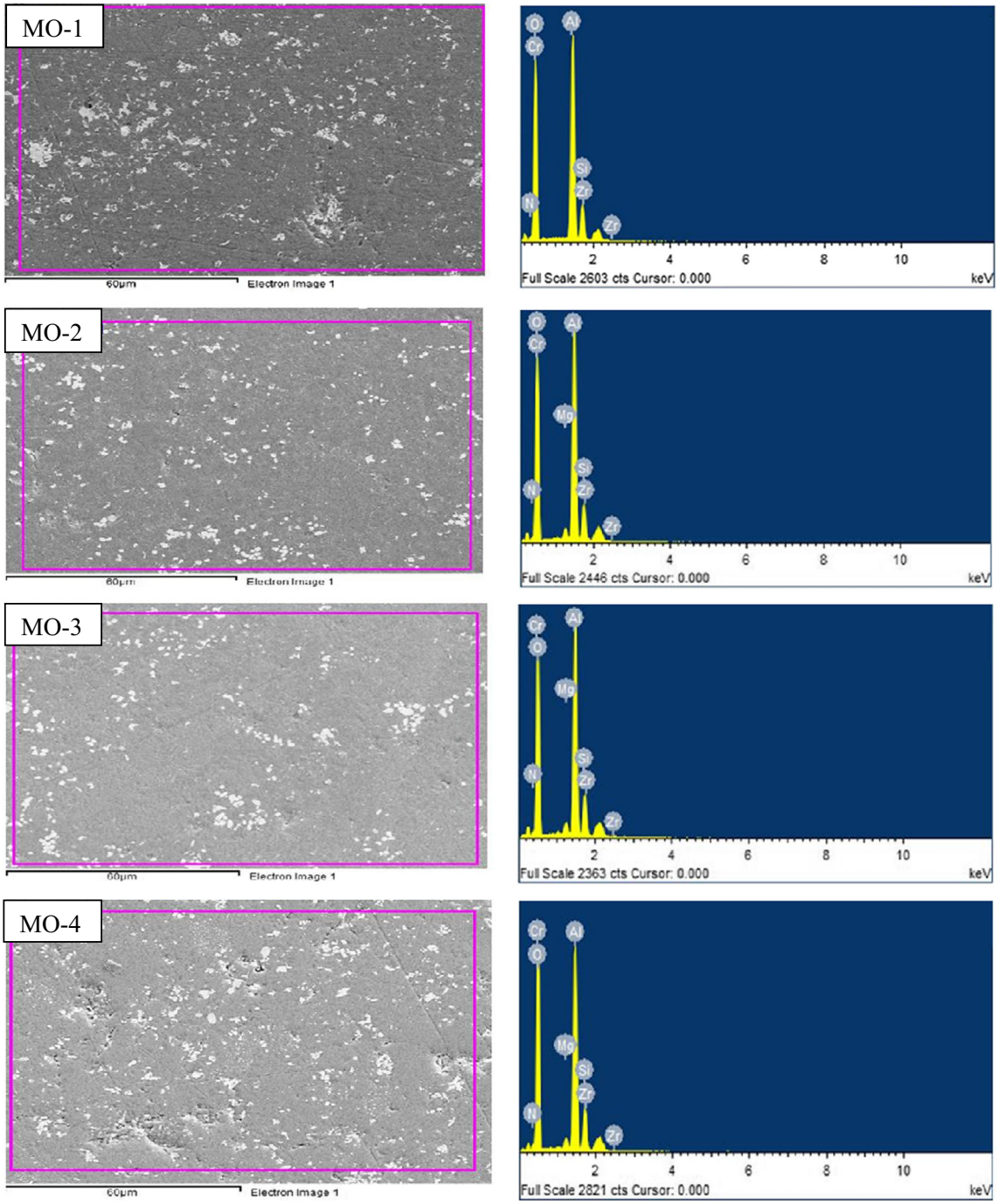

Fig. 4 FESEM images and corresponding EDX spectrum of the composites

whereas the void content of the composites decreases as the amount of MgO increases. There is no much difference in the densities of Al_2O_3 and MgO hence density remains same. The void content of the MgO added composites i.e. MO-2/MO-3/MO-4 remains approximately 29–53% lower than without MgO added composite i.e. MO-1. The lower void content in MgO added composites may be attributed to the fact that MgO form a liquid at higher temperature during sintering process and try to fill the pores [24].

As can be seen in Fig. 7, there were a decrease in indentation depth and an increase in nanohardness of the composites as the content of MgO increased from 0 to 3 wt.% and then indentation depth shows an increasing trend and nanohardness shows a decreasing trend above 3 wt.% of MgO content. The highest nanohardness of 27.83 GPa and lowest indentation depth of 69.61 mm were obtained in the composite MO-3 having 3 wt.% MgO content. For comparison, Zhang et al. [24] obtained a maximum hardness

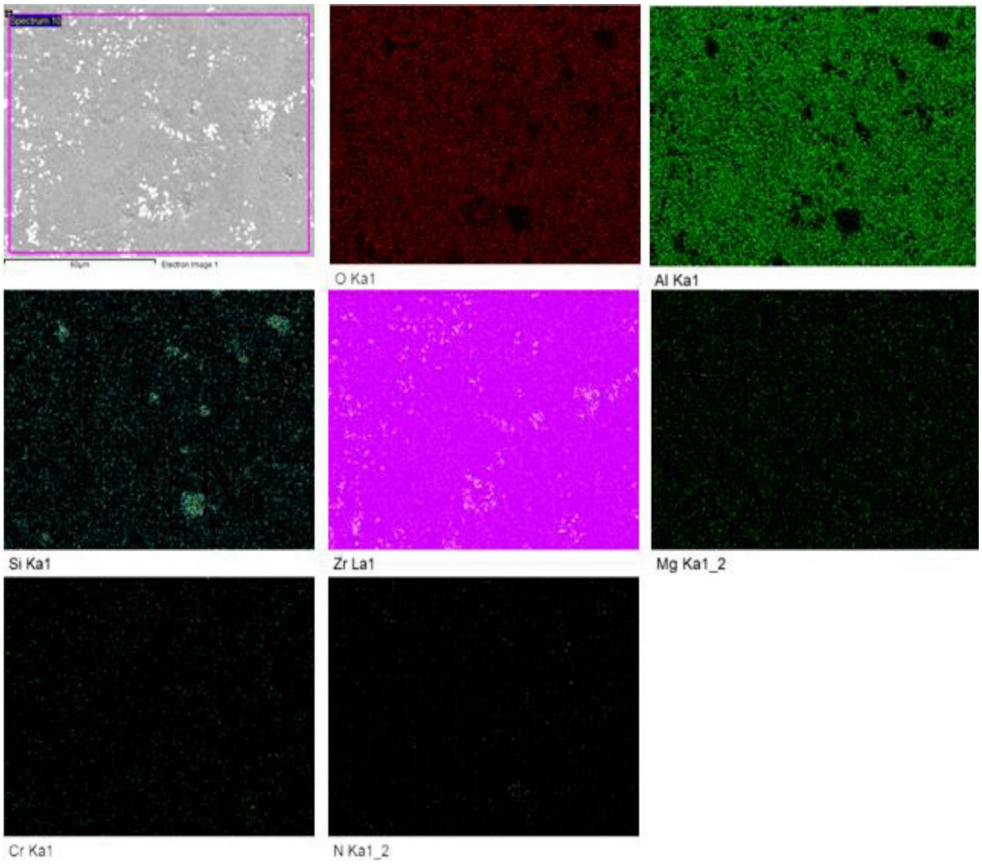

Fig. 5 FESEM elemental mapping of MO-3 composite

of 17.50 GPa for magnesium-oxide and alumina based artificial joints composite. The highest hardness achieved in the present work is much higher to the results of Zhang et al. [24]. The indentation depths for the composites MO-1, MO-2 and MO-4 remains much higher (~85.30 ± 2.38 nm) which could be due to the lower hardness of these composites compared to MO-3 where the indentation depth is much lower and remains ~69.61 nm. The hardness of the composite without adding MgO i.e. MO-1 is lower than others composites. This may be attributed to the fact that MgO added composites reduces the void content and try to promote composites structure [24]. Figure 8 presents the Young's modulus of the fabricated hip implant composites. It can be observed that the Young's modulus

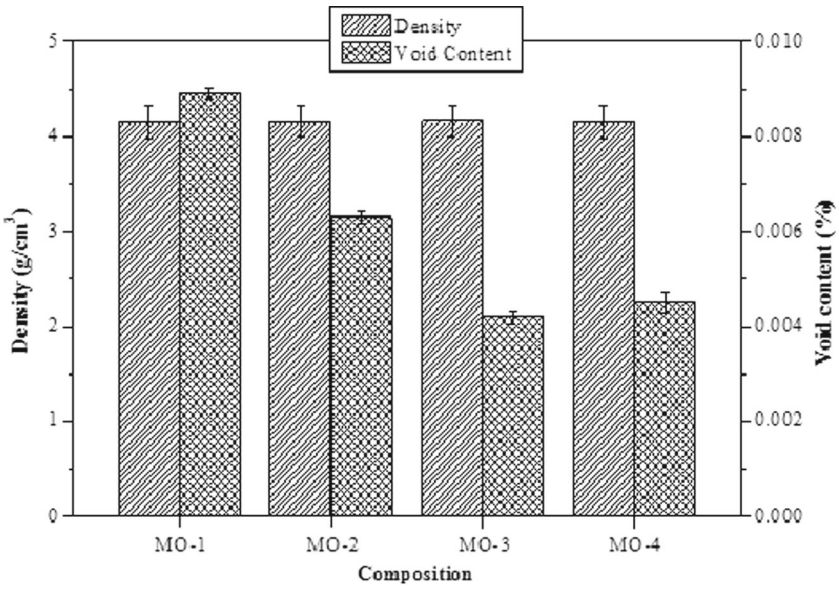

Fig. 6 Density and void content of the composites as a function of composition

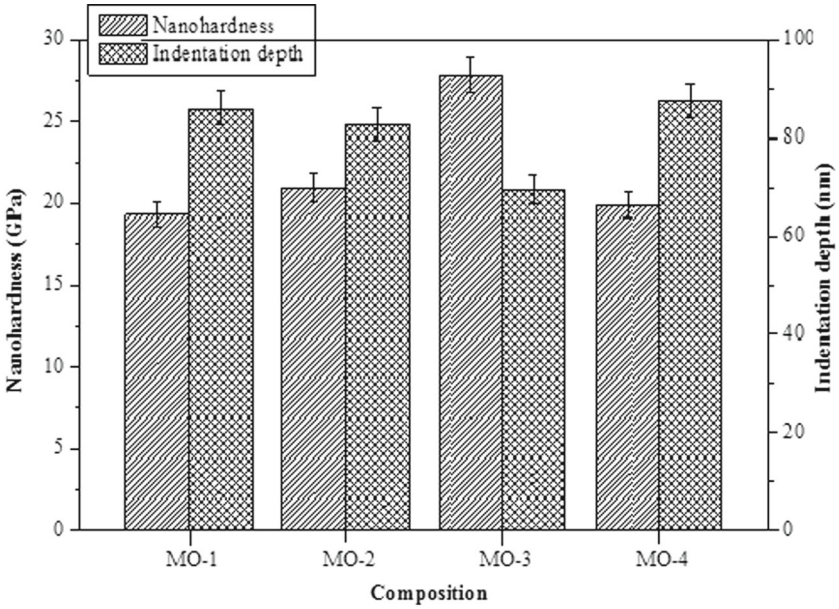

Fig. 7 Nanohadness and indentation depth of the composites as a function of composition

of the MO-1 has been improved slightly for MO-2, by adding 1.5 wt.% MgO and it increased considerably for MO-3 having 3 wt.% MgO. The Young's modulus decreases with the further increase in MgO content. A maximum increase of approximately 14% in Young's modulus was achieved by introducing 3 wt.% MgO content. The Young's modulus of MO-3 composite (~276.55 GPa) remains much higher to that of MO-1/MO-2/MO-4 composites (236.58 ± 7.52 GPa). Similar to indentation depth and nano-hardness, Young's modulus is mainly affected by void content. The lower voids will results in better Young's modulus while the presence of higher voids will allow cracks formation easily due to the concentrations of stresses around the voids.

Fracture toughness of the fabricated hip implant composites is depicted in Fig. 9. For fracture toughness analysis, the composite surfaces were penetrated by a pyramidal indenter with 20N load for 13 s for crack generation. Figure 10 illustrates the effect of indentation on the investigated composites. The shown FESEM images indicate the existence of regular cracks around the indented area.

It is noted that variation in fracture toughness exhibits the same trend as the Young's modulus and all the MgO added composites (i.e. MO-2/MO-3/MO-4) shows improved fracture toughness in comparison with MO-1, the composite without MgO content. A noticeable increase in fracture toughness has been achieved with 3 wt.% MgO

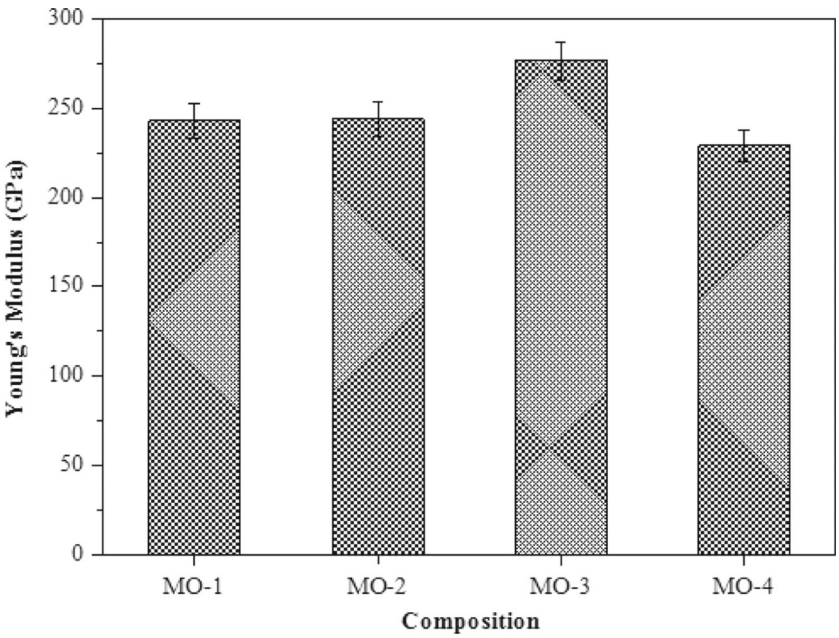

Fig. 8 Young's modulus of the composites as a function of composition

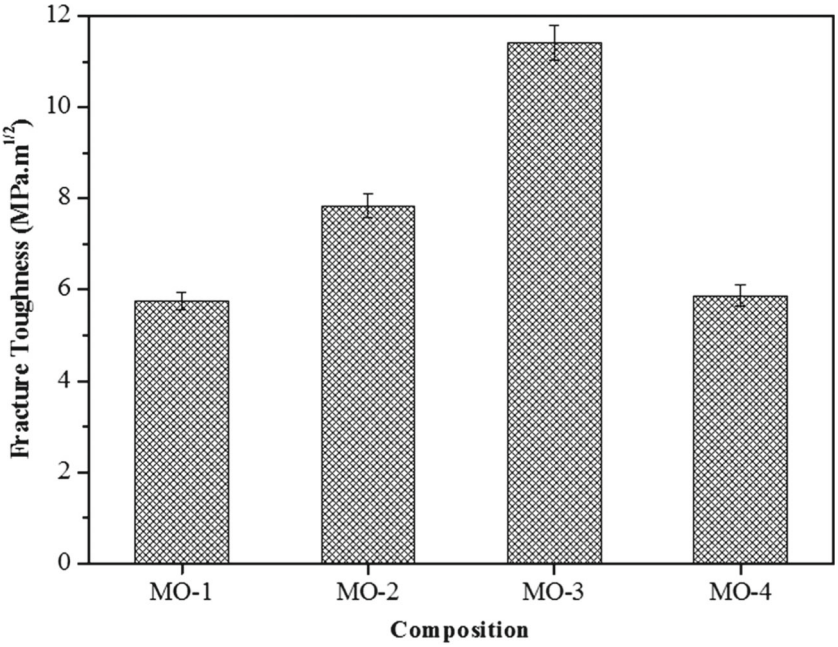

Fig. 9 Fracture toughness of the composites as a function of composition

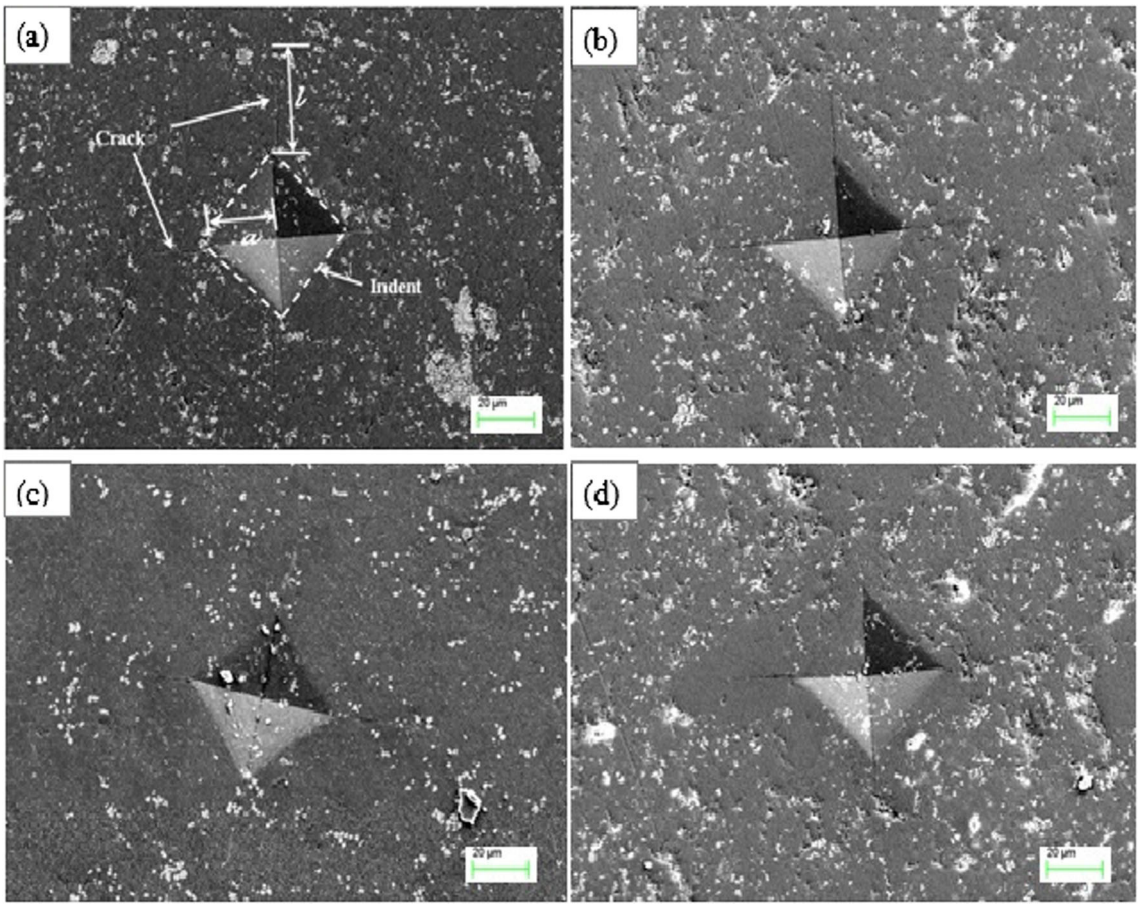

Fig. 10 FESEM images of indentation cracks developed in composites **a** MO-1, **b** MO-2, **c** MO-3 and **d** MO-4

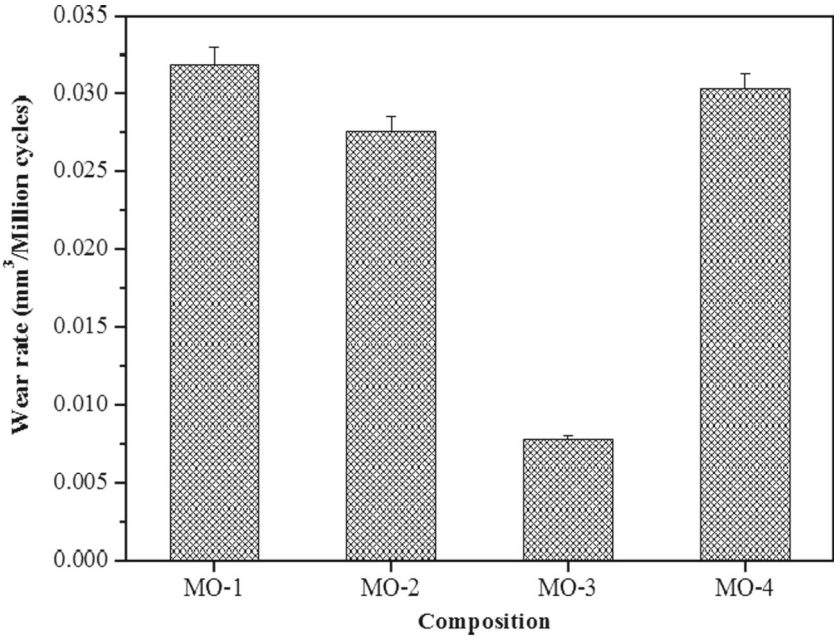

Fig. 11 Wear rate of the composites as a function of composition

content. A further increase in MgO content leads to decrease in fracture toughness. The obtained maximum fracture toughness (11.41 MPa.m$^{1/2}$) for MO-3 having 3 wt.% MgO content is ∼98% higher than that of MO-1 composite having no MgO content. Similar observations have also been reported by Zhang et al. [24] where 12.10 MPa.m$^{1/2}$ fracture toughness registered for magnesium-oxide and alumina based artificial joints composite.

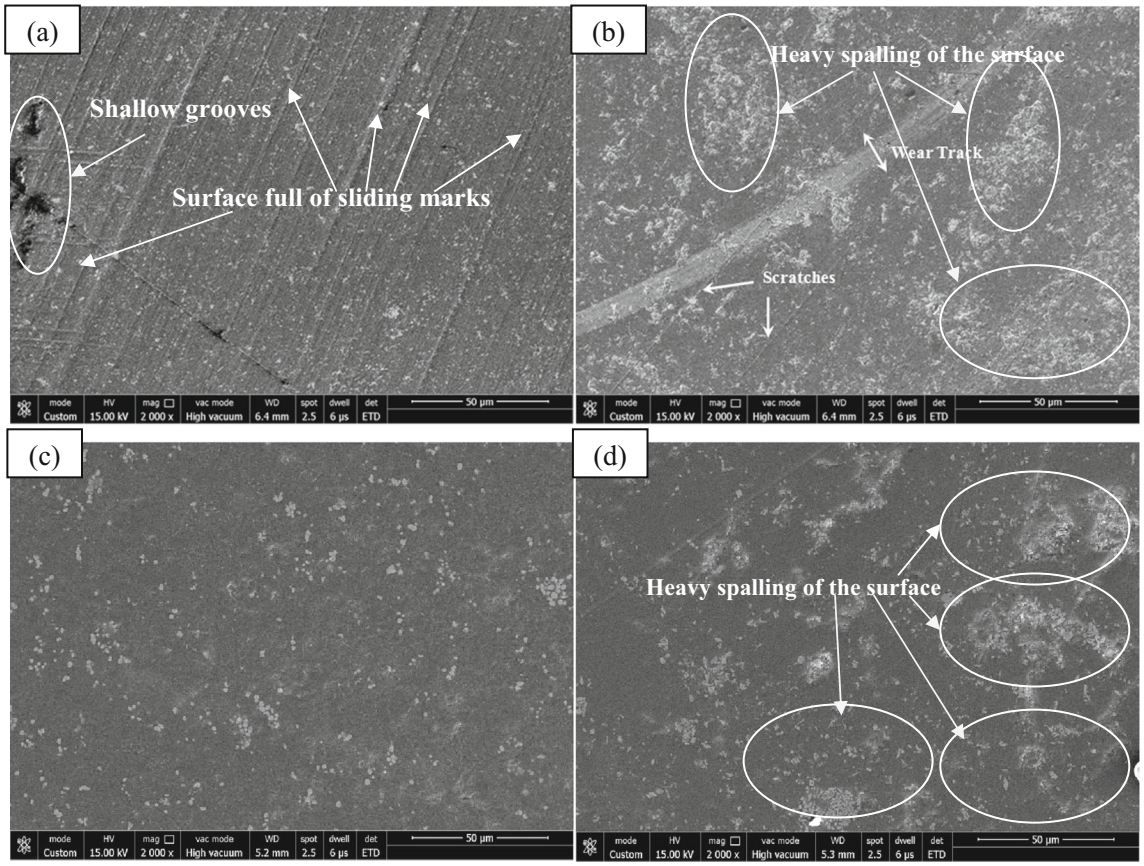

Fig. 12 Worn surface morphologies of the composites **a** MO-1 **b** MO-2 **c** MO-3 **d** MO-4

3.4 Wear Performance

The wear of the investigated composites in relation to composition is depicted in Fig. 11. The results indicated that composites MO-1, MO-2 and MO-4 had wear rate in the range of 0.0276–0.0323 mm^3/million cycles and remains much higher than that of MO-3 (0.0078 mm^3/million cycles). The lower hardness of MO-1/MO-2/MO-4 composites (18.66 ± 2.33 GPa) leading to increased wear compared to that of MO-3 (27.83 GPa). For comparison, Uribe et al. [30] obtained a wear rate of 0.18 mm^3/million cycles for alumina-on-alumina and 0.12 mm^3/million cycles for zirconia toughened alumina-on-alumina, and in a recent work by Amaral et al. [31], wear rate of 0.005 mm^3/million cycles was achieved for nanocrystalline diamond coated ceramic hip joints. The lowest experimental value of wear rate in the present work is much lesser to the results of Uribe et al. [30] and almost 1.5 times higher to the results reported by Amaral et al. [31]. To assess the possible wear mechanism of the composites, the worn surfaces were analyzed using SEM and the morphologies are presented in Fig. 12. The wear tracks of MO-1 (Fig. 12a) showed deep and grooves compared to those observed on MgO added composites (i.e. MO-2/MO-3/MO-4, Fig. 12b–d). The presence of continuous sliding marks on the wear surface can be due to the micro-cutting mechanism which contributed to the severe damage and high material loss of MO-1 composite. The worn surface morphology of MgO filled composites (i.e. MO-2/MO-3/MO-4) was found to be drastically different from that of MO-1. Generally, shear forces produced during wear will leads to spalling of the surface. This spalling was severe in MO-1 composite, as shown in Fig. 12a, most probably due to its lowest hardness. The spalling was observed to be decreased for MO-2/MO-4 (Fig. 12b and d) composites and remains lowest for composite MO-3 (Fig. 12c). The high hardness of MO-3 composite found to provide better wear performance and the worn surface was appeared to be smoother as compared to other investigated composites.

4 Conclusions

In this study, mixed ceramic oxide based hip implant composites containing zirconium oxide, silicon nitride, chromium oxide and varying proportion of aluminum oxide and magnesium oxide were successfully fabricated using a spark plasma sintering process. XRD results suggest that no new product was formed during sintering process. FESEM and EDX results show that starting constituents are present and uniformly distribute in the fabricated hip implant composites. Experimental results indicated that void content, hardness, fracture toughness, Young's modulus and wear performance of these composites were improved by the addition of magnesium oxide content. Magnesium oxide added composites exhibits hardness of 19.93–27.83 GPa, fracture toughness of about 5.89–11.41 $MPam^{1/2}$, Young's modulus of 229.05–276.55 GPa and wear rate of 0.0078–0.0303 mm^3/million cycles, which was superior to many bioceramics. Composites with 3 wt.% added magnesium oxide shows lowest wear rate of 0.0078 mm^3/million cycles in combination with highest hardness, Young's modulus and fracture toughness. Finally, study concludes that 3 wt.% magnesium oxide added composites will be expected to be used in ceramic-on-ceramic hip implant replacements.

References

1. Perrichon A, Reynard B, Gremillard L, Chevalier J, Farizon F, Geringer J (2017) J Mech Behav Biomed Mater 65:600–608
2. Trommer RM, Maru MM (2017) Rev Bras Ortop (English Edition) 52(3):251–259
3. Napier RJ, Shimmin AJ (2016) Semin Arthroplast 27(4):235–238
4. Skinner JA, Haddad FS (2017) Bone Joint J 99-B(8):993–995
5. Yoshitoshi H, Yukiharu H, Taisuke S, Daigo K, Naoki I (2016) J Arthroplasty 31(6):1246–1250
6. Vendittoli PA, Amzica T, Roy AG, Lusignan D, Girard J, Lavigne M (2011) J Arthroplasty 26(2):282–288
7. Smeekes C, Ongkiehong B, van der Wal B, Wolterbeek R, Henseler JF, Nelissen R (2015) Int Orthop 39(4):631–638
8. Lachiewicz PF, Soileau ES, Martell JM (2016) Clin Orthop Relat Res 474(2):365–371
9. Roy T, Choudhury D, Ghosh S, Mamat AB, Murphy BP (2015) Ceram Int Part A 41(1):681–690
10. Boutin P, Christel P, Dorlot JM, Meunier A, Roquancourt A, Blanquaert D, Herman S, Sedel L, Witvoet J (1988) J Biomed Mater Res Part A 22(12):1203–1232
11. Iwakiri K, Iwaki H, Minoda Y, Ohashi H, Takaoka K (2008) Clin Orthop Relat Res 466(5):1186–1192
12. Rahman HS, Choudhury D, Osman NAA, Shasmin HN, Abas WABW (2013) J Ceram Soc Jpn 121(1412):382–387
13. Al-Hajjar M, Carbone S, Jennings LM, Begand S, Oberbach T, Delfosse D, Fisher J (2017) Appl Biomater 105(6):1361–1368
14. Jenabzadeh AR, Pearce SJ, Walter WL (2012) Semin Arthroplast 23(4):232–240
15. Bal BS, Khandkar A, Lakshminarayanan R, Clarke I, Hoffman AA, Rahaman MN (2008) J Biomed Mater Res Part B: Appl Biomater 87(2):447–454
16. Mazzocchi M, Bellosi A (2008) J Mater Sci Mater Med 19(8):2881–2887
17. Mazzocchi M, Bellosi A (2008) J Mater Sci Mater Med 19(8):2889–2901
18. Olofsson J, Grehk TM, Berlind T, Persson C, Jacobson S, Engqvist H (2012) Biomaterials 2:94–102
19. Pettersson M, Bryant M, Schmidt S, Engqvist H, Hall RM, Neville A, Persson C (2016) Mater Sci Eng C 62:497–505
20. Garvie RC, NIcholson PS (1972) J Am Ceram Soc 55(3):152–157
21. Rijal NP, Adhikari U, Khanal S, Pai D, Sankar J, Bhattarai N (2018) Mater Sci Eng B 228:18–27
22. Zhao Y, Liu B, You C, Chen M (2016) Mater Des 89:573–581
23. Karthik K, Dhanuskodi S, Kumar SP, Gobinath C, Sivaramakrishnan S (2017) Mater Lett 206:217–220

24. Zhang Y, Shu Y, Li W, Jiang S, Cao W, Wu Z, Wang K (2017) Ceram Int 43(2):2807–2814
25. Oliver WC, Pharr GM (1992) J Mater Res 7(6):1564–1583
26. Anstis GR, Chantikul P, Lawn BR, Marshall DB (1981) J Am Ceram Soc 64(9):533–538
27. International Standards (2012) ISO-6474-2(en), 2012-04
28. International Standards (2017) ISO-23317 First Edition 06-15
29. Liu J, Yang Y, Hassanin H, Jumbu N, Deng S, Zuo Q, Jiang K (2016) ACS Appl Mater Interfaces 8(4):2607–2616
30. Uribe J, Geringer J, Gremillard L, Reynard B (2013) Tribol Int 63:151–157
31. Amaral M, Maru MM, Rodrigues SP, Gouvêa CP, Trommer RM, Oliveira FJ, Achete CA, Silva RF (2015) Tribol Int 89: 72–77